# Measurement of the energy spectrum of cosmic rays above $10^{18}$ eV using the Pierre Auger Observatory

The Pierre Auger Collaboration[a]

[a] *Observatorio Pierre Auger, Av. San Martin Norte 304, 5613 Malargüe, Argentina*



**Abstract**

We report a measurement of the flux of cosmic rays with unprecedented precision and statistics using the Pierre Auger Observatory. Based on fluorescence observations in coincidence with at least one surface detector we derive a spectrum for energies above $10^{18}$ eV. We also update the previously published energy spectrum obtained with the surface detector array. The two spectra are combined addressing the systematic uncertainties and, in particular, the influence of the energy resolution on the spectral shape. The spectrum can be described by a broken power law $E^{-\gamma}$ with index $\gamma = 3.3$ below the ankle which is measured at $\log_{10}(E_{\rm ankle}/{\rm eV}) = 18.6$. Above the ankle the spectrum is described by a power law with index 2.6 followed by a flux suppression, above about $\log_{10}(E/{\rm eV}) = 19.5$, detected with high statistical significance.

*Keywords:* Pierre Auger Observatory, cosmic rays, energy spectrum

**The Pierre Auger Collaboration**

J. Abraham[8], P. Abreu[73], M. Aglietta[55], E.J. Ahn[89], D. Allard[31], I. Allekotte[1], J. Allen[92], J. Alvarez-Muñiz[80], M. Ambrosio[48], L. Anchordoqui[106], S. Andringa[73], T. Antičić[25], A. Anzalone[54], C. Aramo[48], E. Arganda[77], K. Arisaka[97], F. Arqueros[77], H. Asorey[1], P. Assis[73], J. Aublin[33], M. Ave[37,98], G. Avila[10], T. Bäcker[43], D. Badagnani[6], M. Balzer[38], K.B. Barber[11], A.F. Barbosa[14], S.L.C. Barroso[20], B. Baughman[94], P. Bauleo[87], J.J. Beatty[94], B.R. Becker[103], K.H. Becker[36], A. Bellétoile[34], J.A. Bellido[11], S. BenZvi[105], C. Berat[34], T. Bergmann[38], X. Bertou[1], P.L. Biermann[40], P. Billoir[33], O. Blanch-Bigas[33], F. Blanco[77], M. Blanco[78], C. Bleve[47], H. Blümer[39,37], M. Boháčová[98,27], D. Boncioli[49], C. Bonifazi[23,33], R. Bonino[55], N. Borodai[71], J. Brack[87], P. Brogueira[73], W.C. Brown[88], R. Bruijn[83], P. Buchholz[43], A. Bueno[79], R.E. Burton[85], N.G. Busca[31], K.S. Caballero-Mora[39], L. Caramete[40], R. Caruso[50], A. Castellina[55], O. Catalano[54], G. Cataldi[47], L. Cazon[73,98], R. Cester[51], J. Chauvin[34], A. Chiavassa[55], J.A. Chinellato[18], A. Chou[89,92], J. Chudoba[27], R.W. Clay[11], E. Colombo[2], M.R. Coluccia[47], R. Conceição[73], F. Contreras[9], H. Cook[83], M.J. Cooper[11], J. Coppens[67,69], A. Cordier[32], U. Cotti[65], S. Coutu[95], C.E. Covault[85], A. Creusot[75], A. Criss[95], J. Cronin[98], A. Curutiu[40], S. Dagoret-Campagne[32], R. Dallier[35], K. Daumiller[37], B.R. Dawson[11], R.M. de Almeida[18], M. De Domenico[50], C. De Donato[66,46], S.J. de Jong[67], G. De La Vega[8], W.J.M. de Mello Junior[18], J.R.T. de Mello Neto[23], I. De Mitri[47], V. de Souza[16], K.D. de Vries[68], G. Decerprit[31], L. del Peral[78], O. Deligny[30], A. Della Selva[48], C. Delle Fratte[49], H. Dembinski[41], C. Di Giulio[49], J.C. Diaz[91], M.L. Díaz Castro[15], P.N. Diep[107], C. Dobrigkeit [18], J.C. D'Olivo[66], P.N. Dong[107,30], A. Dorofeev[87], J.C. dos Anjos[14], M.T. Dova[6], D. D'Urso[48], I. Dutan[40], M.A. DuVernois[100], J. Ebr[27], R. Engel[37], M. Erdmann[41], C.O. Escobar[18], A. Etchegoyen[2], P. Facal San Luis[98,80], H. Falcke[67,70], G. Farrar[92], A.C. Fauth[18], N. Fazzini[89], A. Ferrero[2], B. Fick[91], A. Filevich[2], A. Filipčič[74,75], I. Fleck[43], S. Fliescher[41], C.E. Fracchiolla[87], E.D. Fraenkel[68], U. Fröhlich[43], W. Fulgione[55], R.F. Gamarra[2], S. Gambetta[44], B. García[8], D. García Gámez[79], D. Garcia-Pinto[77], X. Garrido[37,32], G. Gelmini[97], H. Gemmeke[38], P.L. Ghia[30,55], U. Giaccari[47], M. Giller[72], H. Glass[89], L.M. Goggin[106], M.S. Gold[103], G. Golup[1], F. Gomez Albarracin[6], M. Gómez Berisso[1], P. Gonçalves[73], D. Gonzalez[39], J.G. Gonzalez[79,90], D. Góra[39,71], A. Gorgi[55], P. Gouffon[17], S.R. Gozzini[83], E. Grashorn[94], S. Grebe[67], M. Grigat[41], A.F. Grillo[56], Y. Guardincerri[4], F. Guarino[48], G.P. Guedes[19], J.D. Hague[103], V. Halenka[28], P. Hansen[6], D. Harari[1], S. Harmsma[68,69], J.L. Harton[87], A. Haungs[37], T. Hebbeker[41], D. Heck[37], A.E. Herve[11], C. Hojvat[89], V.C. Holmes[11], P. Homola[71], J.R. Hörandel[67], A. Horneffer[67], M. Hrabovský[28,27], T. Huege[37], M. Hussain[75], M. Iarlori[45], A. Insolia[50], F. Ionita[98], A. Italiano[50], S. Jiraskova[67], K. Kadija[25], M. Kaducak[89], K.H. Kampert[36], T. Karova[27], P. Kasper[89], B. Kégl[32], B. Keilhauer[37], A. Keivani[90], J. Kelley[67], E. Kemp[18], R.M. Kieckhafer[91], H.O. Klages[37], M. Kleifges[38], J. Kleinfeller[37], R. Knapik[87], J. Knapp[83], D.-H. Koang[34], A. Krieger[2], O. Krömer[38], D. Kruppke-Hansen[36], F. Kuehn[89], D. Kuempel[36], K. Kulbartz[42], N. Kunka[38], A. Kusenko[97], G. La Rosa[54], C. Lachaud[31], B.L. Lago[23], P. Lautridou[35], M.S.A.B. Leão[22], D. Lebrun[34], P. Lebrun[89], J. Lee[97], M.A. Leigui de Oliveira[22], A. Lemiere[30], A. Letessier-Selvon[33], I. Lhenry-Yvon[30], R. López[61], A. Lopez Agüera[80], K. Louedec[32], J. Lozano Bahilo[79], A. Lucero[55], M. Ludwig[39], H. Lyberis[30], M.C. Maccarone[54], C. Macolino[33,45], S. Maldera[55], D. Mandat[27], P. Mantsch[89], A.G. Mariazzi[6], V. Marin[35], I.C. Maris[33,39], H.R. Marquez Falcon[65], G. Marsella[52], D. Martello[47], O. Martínez Bravo[61], H.J. Mathes[37], J. Matthews[90,96], J.A.J. Matthews[103], G. Matthiae[49], D. Maurizio[51], P.O. Mazur[89], M. McEwen[78], G. Medina-Tanco[66], M. Melissas[39], D. Melo[51], E. Menichetti[51], A. Menshikov[38], C. Meurer[41], S. Mičanović[25], M.I. Micheletti[2], W. Miller[103], L. Miramonti[46], S. Mollerach[1], M. Monasor[98,77], D. Monnier Ragaigne[32], F. Montanet[34], B. Morales[66], C. Morello[55], E. Moreno[61], J.C. Moreno[6], C. Morris[94], M. Mostafá[87], S. Mueller[37], M.A. Muller[18], R. Mussa[51], G. Navarra[55 ‡], J.L. Navarro[79], S. Navas[79], P. Necesal[27], L. Nellen[66], P.T. Nhung[107], N. Nierstenhoefer[36], D. Nitz[91], D. Nosek[26], L. Nožka[27], M. Nyklicek[27], J. Oehlschläger[37], A. Olinto[98], P. Oliva[36], V.M. Olmos-Gilbaja[80], M. Ortiz[77], N. Pacheco[78], D. Pakk Selmi-Dei[18], M. Palatka[27], J. Pallotta[3], N. Palmieri[39], G. Parente[80], E. Parizot[31], S. Parlati[56], A. Parra[80], J. Parrisius[39], R.D. Parsons[83], S. Pastor[76], T. Paul[93], V. Pavlidou[98 c], K. Payet[34], M. Pech[27], J. Pękala[71], R. Pelayo[80], I.M. Pepe[21], L. Perrone[52], R. Pesce[44], E. Petermann[102], S. Petrera[45,53], P. Petrinca[49], A. Petrolini[44], Y. Petrov[87], J. Petrovic[69], C. Pfendner[105], R. Piegaia[4], T. Pierog[37], M. Pimenta[73], V. Pirronello[50], M. Platino[2], V.H. Ponce[1], M. Pontz[43], P. Privitera[98], M. Prouza[27], E.J. Quel[3], J. Rautenberg[36], O. Ravel[35], D. Ravignani[2], A. Redondo[78], B. Revenu[35], F.A.S. Rezende[14], J. Ridky[27], S. Riggi[50], M. Risse[43,36], P. Ristori[3], C. Rivière[34], V. Rizi[45], C. Robledo[61], G. Rodriguez[80,49], J. Rodriguez Martino[9,50], J. Rodriguez Rojo[9], I. Rodriguez-Cabo[80], M.D. Rodríguez-Frías[78], G. Ros[78], J. Rosado[77], T. Rossler[28], M. Roth[37], B. Rouillé-d'Orfeuil[98,31], E. Roulet[1], A.C. Rovero[7], F. Salamida[37,45], H. Salazar[61 b], G. Salina[49], F. Sánchez[2,66], M. Santander[9], C.E. Santo[73], E. Santos[73], E.M. Santos[23], F. Sarazin[86], S. Sarkar[81], R. Sato[9], N. Scharf[41], V. Scherini[36], H. Schieler[37], P. Schiffer[41], A. Schmidt[38], F. Schmidt[98], T. Schmidt[39],

O. Scholten[68], H. Schoorlemmer[67], J. Schovancova[27], P. Schovánek[27], F. Schroeder[37], S. Schulte[41], F. Schüssler[37], D. Schuster[86], S.J. Sciutto[6], M. Scuderi[50], A. Segreto[54], D. Semikoz[31], M. Settimo[47], R.C. Shellard[14,15], I. Sidelnik[2], B.B. Siffert[23], G. Sigl[42], A. Śmiałkowski[72], R. Šmída[37,27], G.R. Snow[102], P. Sommers[95], J. Sorokin[11], H. Spinka[84,89], R. Squartini[9], J. Stasielak[71], M. Stephan[41], E. Strazzeri[54,32], A. Stutz[34], F. Suarez[2], T. Suomijärvi[30], A.D. Supanitsky[66], T. Šuša[25], M.S. Sutherland[94], J. Swain[93], Z. Szadkowski[36,72], A. Tamashiro[7], A. Tamburro[39], A. Tapia[2], T. Tarutina[6], O. Taşcău[36], R. Tcaciuc[43], D. Tcherniakhovski[38], D. Tegolo[50,59], N.T. Thao[107], D. Thomas[87], J. Tiffenberg[4], C. Timmermans[69,67], W. Tkaczyk[72], C.J. Todero Peixoto[22], B. Tomé[73], A. Tonachini[51], P. Travnicek[27], D.B. Tridapalli[17], G. Tristram[31], E. Trovato[50], M. Tueros[6], R. Ulrich[95,37], M. Unger[37], M. Urban[32], J.F. Valdés Galicia[66], I. Valiño[37], L. Valore[48], A.M. van den Berg[68], J.R. Vázquez[77], R.A. Vázquez[80], D. Veberič[75,74], T. Venters[98], V. Verzi[49], M. Videla[8], L. Villaseñor[65], S. Vorobiov[75], L. Voyvodic[89 ‡], H. Wahlberg[6], P. Wahrlich[11], O. Wainberg[2], D. Warner[87], A.A. Watson[83], S. Westerhoff[105], B.J. Whelan[11], G. Wieczorek[72], L. Wiencke[86], B. Wilczyńska[71], H. Wilczyński[71], C. Williams[98], T. Winchen[41], M.G. Winnick[11], B. Wundheiler[2], T. Yamamoto[98 a], P. Younk[87], G. Yuan[90], A. Yushkov[48], E. Zas[80], D. Zavrtanik[75,74], M. Zavrtanik[74,75], I. Zaw[92], A. Zepeda[62], M. Ziolkowski[43]

[1] Centro Atómico Bariloche and Instituto Balseiro (CNEA- UNCuyo-CONICET), San Carlos de Bariloche, Argentina
[2] Centro Atómico Constituyentes (Comisión Nacional de Energía Atómica/CONICET/UTN-FRBA), Buenos Aires, Argentina
[3] Centro de Investigaciones en Láseres y Aplicaciones, CITEFA and CONICET, Argentina
[4] Departamento de Física, FCEyN, Universidad de Buenos Aires y CONICET, Argentina
[6] IFLP, Universidad Nacional de La Plata and CONICET, La Plata, Argentina
[7] Instituto de Astronomía y Física del Espacio (CONICET), Buenos Aires, Argentina
[8] National Technological University, Faculty Mendoza (CONICET/CNEA), Mendoza, Argentina
[9] Pierre Auger Southern Observatory, Malargüe, Argentina
[10] Pierre Auger Southern Observatory and Comisión Nacional de Energía Atómica, Malargüe, Argentina
[11] University of Adelaide, Adelaide, S.A., Australia
[14] Centro Brasileiro de Pesquisas Fisicas, Rio de Janeiro, RJ, Brazil
[15] Pontifícia Universidade Católica, Rio de Janeiro, RJ, Brazil
[16] Universidade de São Paulo, Instituto de Física, São Carlos, SP, Brazil
[17] Universidade de São Paulo, Instituto de Física, São Paulo, SP, Brazil
[18] Universidade Estadual de Campinas, IFGW, Campinas, SP, Brazil
[19] Universidade Estadual de Feira de Santana, Brazil
[20] Universidade Estadual do Sudoeste da Bahia, Vitoria da Conquista, BA, Brazil
[21] Universidade Federal da Bahia, Salvador, BA, Brazil
[22] Universidade Federal do ABC, Santo André, SP, Brazil
[23] Universidade Federal do Rio de Janeiro, Instituto de Física, Rio de Janeiro, RJ, Brazil
[25] Rudjer Bošković Institute, 10000 Zagreb, Croatia
[26] Charles University, Faculty of Mathematics and Physics, Institute of Particle and Nuclear Physics, Prague, Czech Republic
[27] Institute of Physics of the Academy of Sciences of the Czech Republic, Prague, Czech Republic
[28] Palacký University, Olomouc, Czech Republic
[30] Institut de Physique Nucléaire d'Orsay (IPNO), Université Paris 11, CNRS-IN2P3, Orsay, France
[31] Laboratoire AstroParticule et Cosmologie (APC), Université Paris 7, CNRS-IN2P3, Paris, France
[32] Laboratoire de l'Accélérateur Linéaire (LAL), Université Paris 11, CNRS-IN2P3, Orsay, France
[33] Laboratoire de Physique Nucléaire et de Hautes Energies (LPNHE), Universités Paris 6 et Paris 7, CNRS-IN2P3, Paris, France
[34] Laboratoire de Physique Subatomique et de Cosmologie (LPSC), Université Joseph Fourier, INPG, CNRS-IN2P3, Grenoble, France
[35] SUBATECH, CNRS-IN2P3, Nantes, France
[36] Bergische Universität Wuppertal, Wuppertal, Germany
[37] Karlsruhe Institute of Technology - Campus North - Institut für Kernphysik, Karlsruhe, Germany
[38] Karlsruhe Institute of Technology - Campus North - Institut für Prozessdatenverarbeitung und Elektronik, Karlsruhe, Germany

[39] Karlsruhe Institute of Technology - Campus South - Institut für Experimentelle Kernphysik (IEKP), Karlsruhe, Germany
[40] Max-Planck-Institut für Radioastronomie, Bonn, Germany
[41] RWTH Aachen University, III. Physikalisches Institut A, Aachen, Germany
[42] Universität Hamburg, Hamburg, Germany
[43] Universität Siegen, Siegen, Germany
[44] Dipartimento di Fisica dell'Università and INFN, Genova, Italy
[45] Università dell'Aquila and INFN, L'Aquila, Italy
[46] Università di Milano and Sezione INFN, Milan, Italy
[47] Dipartimento di Fisica dell'Università del Salento and Sezione INFN, Lecce, Italy
[48] Università di Napoli "Federico II" and Sezione INFN, Napoli, Italy
[49] Università di Roma II "Tor Vergata" and Sezione INFN, Roma, Italy
[50] Università di Catania and Sezione INFN, Catania, Italy
[51] Università di Torino and Sezione INFN, Torino, Italy
[52] Dipartimento di Ingegneria dell'Innovazione dell'Università del Salento and Sezione INFN, Lecce, Italy
[53] Gran Sasso Center for Astroparticle Physics, Italy
[54] Istituto di Astrofisica Spaziale e Fisica Cosmica di Palermo (INAF), Palermo, Italy
[55] Istituto di Fisica dello Spazio Interplanetario (INAF), Università di Torino and Sezione INFN, Torino, Italy
[56] INFN, Laboratori Nazionali del Gran Sasso, Assergi (L'Aquila), Italy
[59] Università di Palermo and Sezione INFN, Catania, Italy
[61] Benemérita Universidad Autónoma de Puebla, Puebla, Mexico
[62] Centro de Investigación y de Estudios Avanzados del IPN (CINVESTAV), México, D.F., Mexico
[65] Universidad Michoacana de San Nicolas de Hidalgo, Morelia, Michoacan, Mexico
[66] Universidad Nacional Autonoma de Mexico, Mexico, D.F., Mexico
[67] IMAPP, Radboud University, Nijmegen, Netherlands
[68] Kernfysisch Versneller Instituut, University of Groningen, Groningen, Netherlands
[69] NIKHEF, Amsterdam, Netherlands
[70] ASTRON, Dwingeloo, Netherlands
[71] Institute of Nuclear Physics PAN, Krakow, Poland
[72] University of Łódź, Łódź, Poland
[73] LIP and Instituto Superior Técnico, Lisboa, Portugal
[74] J. Stefan Institute, Ljubljana, Slovenia
[75] Laboratory for Astroparticle Physics, University of Nova Gorica, Slovenia
[76] Instituto de Física Corpuscular, CSIC-Universitat de València, Valencia, Spain
[77] Universidad Complutense de Madrid, Madrid, Spain
[78] Universidad de Alcalá, Alcalá de Henares (Madrid), Spain
[79] Universidad de Granada & C.A.F.P.E., Granada, Spain
[80] Universidad de Santiago de Compostela, Spain
[81] Rudolf Peierls Centre for Theoretical Physics, University of Oxford, Oxford, United Kingdom
[83] School of Physics and Astronomy, University of Leeds, United Kingdom
[84] Argonne National Laboratory, Argonne, IL, USA
[85] Case Western Reserve University, Cleveland, OH, USA
[86] Colorado School of Mines, Golden, CO, USA
[87] Colorado State University, Fort Collins, CO, USA
[88] Colorado State University, Pueblo, CO, USA
[89] Fermilab, Batavia, IL, USA
[90] Louisiana State University, Baton Rouge, LA, USA
[91] Michigan Technological University, Houghton, MI, USA
[92] New York University, New York, NY, USA
[93] Northeastern University, Boston, MA, USA
[94] Ohio State University, Columbus, OH, USA
[95] Pennsylvania State University, University Park, PA, USA

[96] Southern University, Baton Rouge, LA, USA
[97] University of California, Los Angeles, CA, USA
[98] University of Chicago, Enrico Fermi Institute, Chicago, IL, USA
[100] University of Hawaii, Honolulu, HI, USA
[102] University of Nebraska, Lincoln, NE, USA
[103] University of New Mexico, Albuquerque, NM, USA
[105] University of Wisconsin, Madison, WI, USA
[106] University of Wisconsin, Milwaukee, WI, USA
[107] Institute for Nuclear Science and Technology (INST), Hanoi, Vietnam

(‡) Deceased
(a) at Konan University, Kobe, Japan
(b) On leave of absence at the Instituto Nacional de Astrofisica, Optica y Electronica
(c) at Caltech, Pasadena, USA

## 1. Introduction

The flux of ultra-high energy cosmic rays exhibits two important features. At energies above $4 \times 10^{19}$ eV a suppression of the flux with respect to a power law extrapolation is found [1, 2], which is compatible with the predicted Greisen-Zatsepin-Kuz'min (GZK) effect [3, 4], but could also be related to the maximum energy that can be reached at the sources. A break in the power law, called the ankle, is observed at an energy of about $3 \times 10^{18}$ eV [5, 6, 7, 8]. This break in the energy spectrum has traditionally been attributed to the transition from the galactic component of the cosmic ray flux to a flux dominated by extragalactic sources [9, 10]. In recent years it became clear that a similar feature in the cosmic ray spectrum could also result from the propagation of protons from extragalactic sources, placing the transition from galactic to extragalactic cosmic rays at a much lower energy [11, 12]. In this model the ankle is produced by the modification of the source spectrum of primary protons. This is caused by $e^{\pm}$ pair production of protons with the photons of the cosmic microwave background, leading to a well-defined prediction of the shape of the flux in the ankle region.

Accurate measurement of the cosmic ray flux in the ankle region is expected to help determine the energy range of the transition between galactic and extragalactic cosmic rays and to constrain model scenarios.

Two complementary techniques are used at the Pierre Auger Observatory to detect extensive air showers initiated by ultra-high energy cosmic rays (UHECR): a *surface detector array (SD)* and a *fluorescence detector (FD)*. The SD of the southern observatory in Argentina consists of an array of 1600 water Cherenkov detectors covering an area of about 3000 km$^2$ on a triangular grid with 1.5 km spacing. Electrons, photons and muons in air showers are sampled at ground level with a on-time of almost 100 %. In addition the atmosphere above the surface detector is observed during clear, dark nights by 24 optical telescopes grouped in 4 buildings. These detectors are used to observe the longitudinal development of extensive air showers by detecting the fluorescence light emitted by excited nitrogen molecules and the Cherenkov light induced by the shower particles. Details of the design and status of the Observatory are given elsewhere [13, 14, 15].

The energy spectrum of ultra-high energy cosmic rays at energies greater than $2.5 \times 10^{18}$ eV has been derived using data from the surface detector array of the Pierre Auger Observatory [2]. This measurement provided evidence for the suppression of the flux above $4 \times 10^{19}$ eV and is updated here. In this work we extend the previous measurements to lower energies by analysing air showers measured with the fluorescence detector that also triggered at least one of the stations of the surface detector array. Despite the limited event statistics due to the fluorescence detector on-time of about 13 %, the lower energy threshold and the good energy resolution of these *hybrid* events allow us to measure the flux of cosmic rays in the region of the ankle.

The energy spectrum of hybrid events is determined from data taken between November 2005 and May 2008, during which the Auger Observatory was still under construction. Using selection criteria that are set out below, the exposure accumulated during this period was computed and the flux of cosmic rays above $10^{18}$ eV determined. The spectrum obtained with the surface detector array, updated using data until the end of December 2008, is combined with the hybrid one to obtain a spectrum measurement over a wide energy range with the highest statistics available.

## 2. Hybrid energy spectrum

The hybrid approach to shower observation is based on the shower detection with the FD in coincidence with at least one SD station. The latter condition, though insufficient to establish an independent SD trigger [2, 16], enables the shower geometry and consequently the energy of the primary particle to be determined accurately. The reconstruction accuracy of hybrid events is much better than what can be achieved using SD or FD data independently [17]. For example, the energy resolution of these hybrid measurements is better than 6% above $10^{18}$ eV compared with about 15% for the surface detector data.

Event reconstruction proceeds in two steps. First the shower geometry is found by combining information from the shower image and timing measured with the FD with the trigger time of the surface detector station that has the largest signal [18]. In the second step the profile of energy deposition of the shower is reconstructed [19] and shower parameters such as depth of shower maximum and primary particle energy are calculated together with their uncertainties.

### *2.1. Event selection and reconstruction*

To ensure good energy reconstruction only events that satisfy the following quality criteria are accepted:

- Showers must have a reconstructed zenith angle smaller than 60 °.

- In the plane perpendicular to the shower axis, the reconstructed shower core must be within 1500 m of the station used for the geometrical reconstruction.
- The contribution of Cherenkov light to the overall signal of the FD must be less than 50 %.
- The Gaisser-Hillas fit [19, 20] of the reconstructed longitudinal profile must be successful with $\chi^2/\mathrm{Ndof} < 2.5$.
- The maximum of the shower development, $X_{\mathrm{max}}$, must be observed in the field of view of the telescopes.
- The uncertainty in the reconstructed energy, which includes light flux and geometrical uncertainties, must be $\sigma(E)/E < 20\,\%$.
- Only periods during which no clouds were detected above the Observatory are used.

To avoid a possible bias in event selection due to the differences between shower profiles initiated by primaries of different mass, only showers with geometries that would allow the observation of all primaries in the range from proton to iron are retained in the data sample. The corresponding fiducial volume in shower-telescope distance and zenith angle range is defined as a function of the reconstructed energy and has been verified with data [21]. About 1700 events fulfil the selection criteria for quality and for fiducial volume.

A detailed simulation of the detector response has shown that every FD trigger above $E = 10^{18}$ eV passing all the described selection criteria is accompanied by a SD trigger of at least one station, independent of the mass and direction of the incoming primary particle [22].

### 2.2. Exposure calculation

During the time period discussed here the southern Auger Observatory was in its construction phase with the number of available SD stations increasing from around 630 to a nearly fully completed instrument with 1600 detectors. Over the same period the FD was enlarged from 12 to 24 telescopes. In addition to these large scale changes, smaller but important changes occur on much shorter timescales due, for example, to hardware failures. The data-taking of the fluorescence detector is furthermore influenced by weather effects such as storms or rainfall. These and other factors that affect the efficiency of the data-taking must be taken into account in the determination of the aperture.

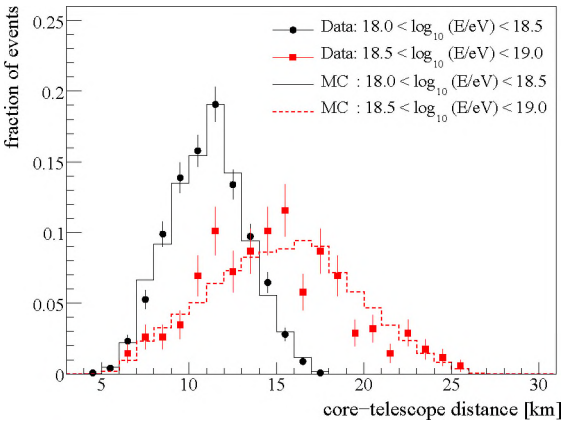


Figure 1: Distribution of events observed with the fluorescence detector as a function of the distance of the shower core from the telescopes for data and Monte Carlo simulation.

The total exposure is the integral over the instantaneous aperture and can be written as

$$\mathcal{E}(E) = \int_T \int_\Omega \int_{S_{\mathrm{gen}}} \varepsilon(E, t, \theta, \phi, x, y)\, \cos\theta\, \mathrm{d}S\, \mathrm{d}\Omega\, \mathrm{d}t, \quad (1)$$

where $\mathrm{d}\Omega = \sin\theta \mathrm{d}\theta \mathrm{d}\phi$ and $\Omega$ are respectively the differential and total solid angles, $\theta$ and $\phi$ are the zenith and azimuth angles and $\mathrm{d}S = \mathrm{d}x \times \mathrm{d}y$ is the horizontal surface element. The final selection efficiency $\varepsilon$ includes the efficiencies of the various steps of the analysis, namely the trigger, reconstruction and selection efficiencies and also the evolution of the detector during the time period $T$. It has been derived from Monte Carlo simulations that scan an area $S_{\mathrm{gen}}$ large enough to enclose the full detector array.

The changing configuration of the SD array is taken into account for the determination of the hybrid on-time. In addition, within time intervals of 10 min, the status of all detector components of the Pierre Auger Observatory down to the level of single PMTs of the fluorescence detector is determined. Moreover all known inefficiencies such as DAQ read-out deadtimes are considered.

The longitudinal profile of the deposition of energy simulated with the QGSJet-II [23, 24] and Sibyll 2.1 [25, 26] hadronic interaction models and the CONEX [27] air shower simulation program are the basis for an extensive set of Monte Carlo simulations. The exact data taking conditions are reproduced by means of a detailed detector simulation within the Auger analysis framework [28]. All atmospheric measurements, e.g.

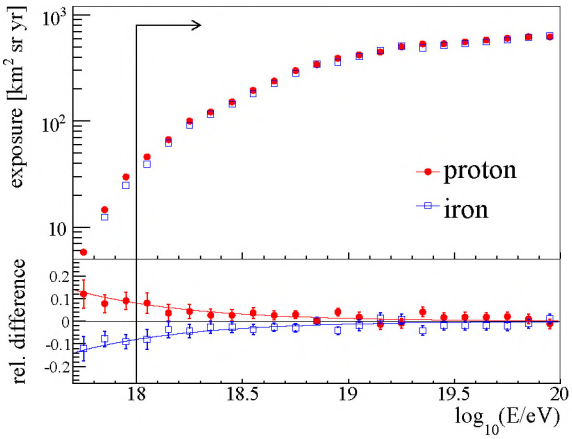


Figure 2: The hybrid exposure for different primary particles together with the difference to the mixed composition used for the flux measurement.

scattering and absorption lengths, as well as monitoring information such as the noise caused by night sky background light and PMT trigger thresholds are taken into account.

The reconstruction of the simulated showers is then performed in exactly the same way as for the data and good agreement between data and Monte Carlo simulations is obtained. As an example, we show in Fig. 1 the distribution of events observed with the fluorescence detector as a function of the distance of the shower core from the telescopes.

Fig. 2 shows the hybrid exposure of events fulfilling all of the quality and fiducial volume cuts that have been applied, for proton and iron primaries. As can be seen, the cuts adopted lead to only a small dependence of the exposure on the mass composition which can be assumed to be dominated by hadrons [29, 30]. The systematic uncertainty arising from our lack of knowledge of the mass composition is about 8% at $10^{18}$ eV and decreases to less than 1% above $10^{19}$ eV. We assume a mixed composition of 50 % proton and 50 % iron nuclei for the flux determination and include the remaining composition dependence in the systematic uncertainty. The dependence of the exposure on the assumed model of hadronic interactions was found to be less than 2% over all the energy range.

The full MC simulation chain has been cross-checked with air shower observations and the analysis of laser shots that are fired from the Central Laser Facility [31] and detected with the fluorescence detector. Following this analysis the exposure has been reduced by 8% to account for lost events and an upper limit to the remaining systematic uncertainty of 5 % was derived [32]. By combination with the uncertainty related to mass composition the total systematic uncertainty of the hybrid exposure is estimated as 10 % (6 %) at $10^{18}$ eV ($> 10^{19}$ eV).

### 2.3. Energy spectrum from hybrid data

The flux of cosmic rays $J$ as a function of energy is given by

$$J(E) = \frac{\mathrm{d}^4 N_{\mathrm{inc}}}{\mathrm{d}E\,\mathrm{d}A\,\mathrm{d}\Omega\,\mathrm{d}t} \cong \frac{\Delta N_{\mathrm{sel}}(E)}{\Delta E}\frac{1}{\mathcal{E}(E)}\,, \qquad (2)$$

where $N_{\mathrm{inc}}$ is the number of cosmic rays with energy $E$ incident on a surface element $\mathrm{d}A$, within a solid angle $\mathrm{d}\Omega$ and time $\mathrm{d}t$. $\Delta N_{\mathrm{sel}}(E)$ is the number of detected events passing the quality cuts in the energy bin centered around $E$ and having width $\Delta E$. $\mathcal{E}(E)$ is the energy-dependent exposure defined above.

The measured flux as function of energy is shown in Fig. 3. A break in the power law of the derived energy spectrum is clearly visible. The position of this feature, known as the ankle, has been determined by fitting two power laws $J = kE^{-\gamma}$ with a free break between them in the energy interval from $10^{18}$ eV to $10^{19.5}$ eV. The upper end of this interval was defined by the flux suppression observed in the spectrum derived using surface detector data [2]. The ankle is found at $\log_{10}(E_{\mathrm{ankle}}/\mathrm{eV}) = 18.65 \pm 0.09(\mathrm{stat})^{+0.10}_{-0.11}(\mathrm{sys})$ and the two power law indices have been determined as $\gamma_1 = 3.28 \pm 0.07(\mathrm{stat})^{+0.11}_{-0.10}(\mathrm{sys})$ and $\gamma_2 = 2.65 \pm 0.14(\mathrm{stat})^{+0.16}_{-0.14}(\mathrm{sys})$, ($\chi^2/\mathrm{ndof} = 10.2/11$), where the systematic uncertainty is due to the residual effect of the unknown mass composition.

The energy estimation of fluorescence measurements relies on the knowledge of the fluorescence yield. Here we adopt the same absolute calibration [33] and the wavelength and pressure dependence [34] as in Ref. [2]. This is currently one of the dominant sources of systematic uncertainty (14 %). The fraction of the energy of the primary particle that is carried by muons and neutrinos and does not contribute to the fluorescence signal has been calculated based on air shower simulations and goes from about 14 % at $10^{18}$ eV to about 10 % at $10^{19}$ eV [35]. The systematic uncertainty depending on the choice of models and mass composition is about 8 % [36]. Further systematic uncertainties in the absolute energy scale are related to the absolute detector calibration (9.5 %) and its wavelength dependence (3 %) [37]. Uncertainties of the lateral width of the shower image and other reconstruction uncertainties amount to about 10 % systematic uncertainty in the energy determination. Atmospheric conditions play a crucial role for air shower observations with fluorescence

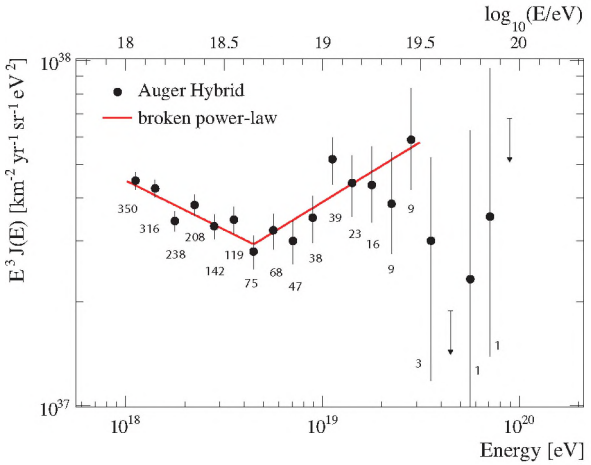


Figure 3: The energy spectrum of ultra-high energy cosmic rays determined from hybrid measurements of the Pierre Auger Observatory. The number of events is given for each of the energy bins next to the corresponding data point. Only statistical uncertainties are shown. The upper limits correspond to the 68% CL. A fit with a broken power law is used to determine the position of the ankle.

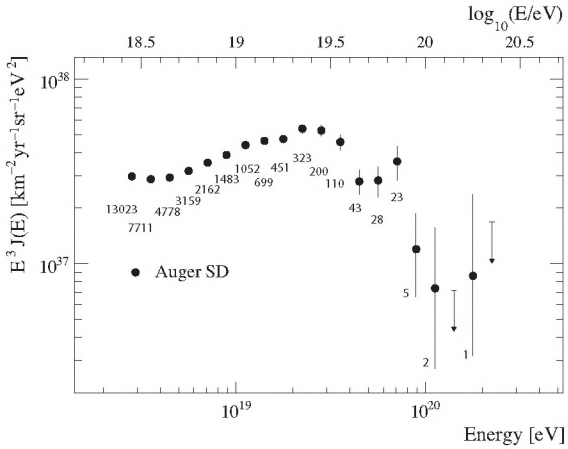


Figure 4: Energy spectrum, corrected for energy resolution, derived from surface detector data calibrated with fluorescence measurements. The number of events is given for each of the energy bins next to the corresponding data point. Only statistical uncertainties are shown. The upper limits correspond to 68% CL.

detectors. An extensive program of atmospheric monitoring is conducted at the Pierre Auger Observatory allowing the determination of the relevant parameters and the associated uncertainties [31, 38, 39, 40]. The total systematic uncertainty in the energy determination is estimated as 22 % [41]. Indirect methods of determining the energy scale, which do not involve the fluorescence detector calibration, seem to indicate an energy normalization that is higher than the one used here by an amount comparable to the uncertainty given above [42].

## 3. Update of Surface Detector Spectrum

Here we update the published energy spectrum based on surface detector data [2] using data until the end of December 2008. The exposure is now 12, 790 km$^2$ sr yr. The event selection requires that the detector station with the highest signal be surrounded by operational stations and that the reconstructed zenith angle be smaller than 60° [16]. More than 35, 000 events fulfill these criteria.

The energy estimator of the surface detector is corrected for shower attenuation effects using a constant-intensity method. The calibration of this energy estimator with fluorescence measurements has been updated using the increased data set of high-quality hybrid events [41].

Because of the energy resolution of the surface detector data (about 20% at the lowest energies, improving to about 10% at the highest energies), bin-to-bin migrations influence the reconstruction of the flux and spectral shape. To correct for these effects, a forward-folding approach is applied. MC simulations are used to determine the energy resolution of the surface detector and a bin-to-bin migration matrix is derived. The matrix is then used to find a flux parameterisation that matches the measured data after forward-folding. The ratio of this parameterisation to the folded flux gives a correction factor that is applied to the data. The correction to the flux is mildly energy dependent and is less than 20% over the full energy range. Details will be discussed in a forthcoming publication.

The energy spectrum, after correction for the energy resolution, is shown in Fig. 4 together with the event numbers of the underlying raw distribution. Combining the systematic uncertainties of the exposure (3%) and of the forward folding assumptions (5%), the systematic uncertainty of the derived flux is 6%.

## 4. The Combined Auger spectrum

The energy spectrum derived from hybrid data is combined with the one obtained from surface detector data using a maximum likelihood method. Since the surface detector energy estimator is calibrated with hybrid events, the two spectra have the same systematic uncertainty in the energy scale. On the other hand, the normalisation uncertainties are independent. They are taken as 6 % for the SD and 10 % (6 %) for the hybrid

Table 1: Fitted parameters and their statistical uncertainties characterising the combined energy spectrum.

| parameter | power laws | power laws + smooth function |
|---|---|---|
| $\gamma_1 (E < E_{\rm ankle})$ | $3.26 \pm 0.04$ | $3.26 \pm 0.04$ |
| $\log_{10}(E_{\rm ankle}/{\rm eV})$ | $18.61 \pm 0.01$ | $18.60 \pm 0.01$ |
| $\gamma_2 (E > E_{\rm ankle})$ | $2.59 \pm 0.02$ | $2.55 \pm 0.04$ |
| $\log_{10}(E_{\rm break}/{\rm eV})$ | $19.46 \pm 0.03$ | |
| $\gamma_3 (E > E_{\rm break})$ | $4.3 \pm 0.2$ | |
| $\log_{10}(E_{1/2}/{\rm eV})$ | | $19.61 \pm 0.03$ |
| $\log_{10}(W_c/{\rm eV})$ | | $0.16 \pm 0.03$ |
| $\chi^2$/ndof | 38.5/16 | 29.1/16 |

flux at $10^{18}$ eV ($> 10^{19}$ eV). These normalisation uncertainties are used as additional constraints in the combination. This combination procedure is used to derive the scale parameters, $k$, for the fluxes that are to be applied to the individual spectra. These are $k_{\rm SD} = 1.01$ and $k_{\rm FD} = 0.99$ for the surface detector data and hybrid data respectively, showing that agreement between the measurements is at the 1% level.

The combined energy spectrum scaled with $E^3$ is shown in Fig. 5 in comparison with the spectrum obtained with stereo measurements of the HiRes instrument [43]. An energy shift within the current systematic uncertainties of the energy scale applied to one or both experiments could account for most of the difference between the spectra. The ankle feature seems to be somewhat more sharply defined in the Auger data. This is possibly due to a systematic energy offset between the experiments. However, for a complete comparison, care must also be taken to account for energy resolution and possible changes in aperture with energy.

The characteristic features of the combined spectrum are quantified in two ways. For the first method, shown as a dotted red line in Fig. 5, we have used three power laws with free breaks between them. A continuation of the power law above the ankle to highest energies can be rejected with more than 20 $\sigma$. For the second characterisation we have adopted two power laws in the ankle region and a smoothly changing function at higher energies which is given by

$$J(E; E > E_{\rm ankle}) \propto \frac{E^{-\gamma_2}}{1 + \exp\left(\frac{\log_{10} E - \log_{10} E_{1/2}}{\log_{10} W_c}\right)}, \qquad (3)$$

where $E_{1/2}$ is the energy at which the flux has fallen to one half of the value of the power-law extrapolation and $W_c$ parametrizes the width of the transition region. It is shown as a black solid line in Fig. 5. The derived parameters (quoting only statistical uncertainties) are given in Tab. 1.

At high energies the combined spectrum is statistically dominated by the surface detector data. The agreement between the index of the power law above the ankle, $\gamma_2$, measured with the combined spectrum ($2.59 \pm 0.02$) and with hybrid data ($2.65 \pm 0.14$), also demonstrates the good agreement between the two measurements.

## 5. Summary

We have measured the cosmic ray flux with the Pierre Auger Observatory by applying two different techniques. The fluxes obtained with hybrid events and from the surface detector array are in good agreement in the overlapping energy range. A combined spectrum has been derived with high statistics covering the energy range from $10^{18}$ eV to above $10^{20}$ eV. The dominant systematic uncertainty of the spectrum stems from that of the overall energy scale, which is estimated to be 22%.

The position of the ankle at $\log_{10}(E_{\rm ankle}/{\rm eV}) = 18.61 \pm 0.01$ has been determined by fitting the flux with a broken power law $E^{-\gamma}$. An index of $\gamma = 3.26 \pm 0.04$ is found below the ankle. Above the ankle the spectrum follows a power law with index $2.55 \pm 0.04$. In comparison to the power law extrapolation, the spectrum is suppressed by a factor two at $\log_{10}(E_{1/2}/{\rm eV}) = 19.61 \pm 0.03$. The significance of the suppression is larger than $20\,\sigma$. The suppression is similar to what is expected from the GZK effect for protons or nuclei as heavy as iron, but could in part also be related to a change of the shape of the average injection spectrum at the sources.

**Acknowledgements.** The successful installation and commissioning of the Pierre Auger Observatory would not have been possible without the strong commitment and effort from the technical and administrative staff in Malargüe.

We are very grateful to the following agencies and organizations for financial support: Comisión Nacional de Energía Atómica, Fundación Antorchas, Gobierno De La Provincia de Mendoza, Municipalidad de Malargüe, NDM Holdings and Valle Las Leñas, in gratitude for their continuing cooperation over land access, Argentina; the Australian Research Council; Conselho Nacional de Desenvolvimento Científico e Tecnológico

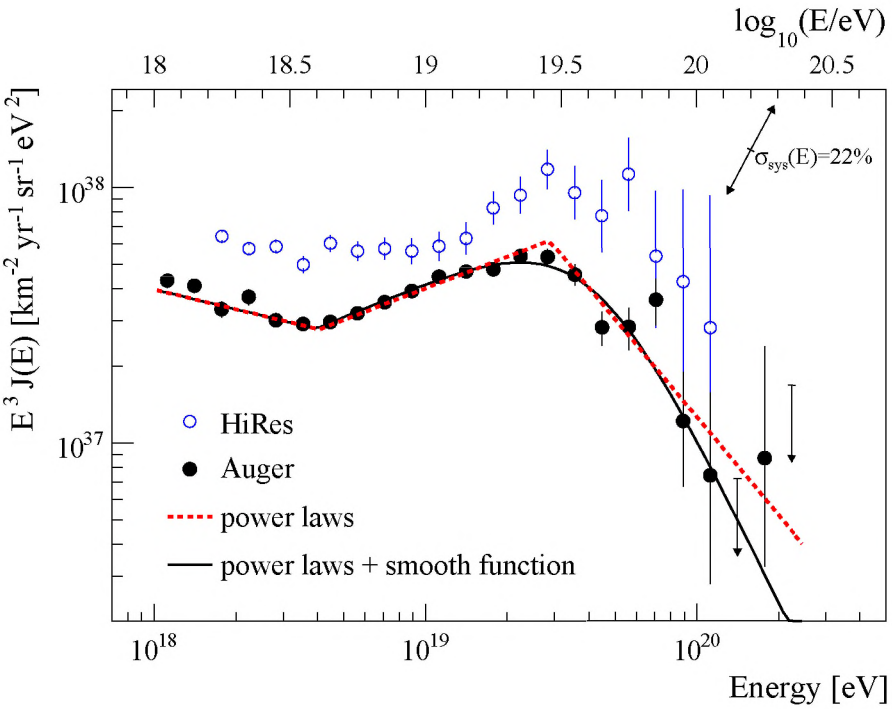


Figure 5: The combined energy spectrum is fitted with two functions (see text) and compared to data from the HiRes instrument [43]. The systematic uncertainty of the flux scaled by $E^3$ due to the uncertainty of the energy scale of 22% is indicated by arrows. A table with the Auger flux values can be found at [44].

(CNPq), Financiadora de Estudos e Projetos (FINEP), Fundação de Amparo à Pesquisa do Estado de Rio de Janeiro (FAPERJ), Fundação de Amparo à Pesquisa do Estado de São Paulo (FAPESP), Ministério de Ciência e Tecnologia (MCT), Brazil; AVCR AV0Z10100502 and AV0Z10100522, GAAV KJB300100801 and KJB100100904, MSMT-CR LA08016, LC527, 1M06002, and MSM0021620859, Czech Republic; Centre de Calcul IN2P3/CNRS, Centre National de la Recherche Scientifique (CNRS), Conseil Régional Ile-de-France, Département Physique Nucléaire et Corpusculaire (PNC-IN2P3/CNRS), Département Sciences de l'Univers (SDU-INSU/CNRS), France; Bundesministerium für Bildung und Forschung (BMBF), Deutsche Forschungsgemeinschaft (DFG), Finanzministerium Baden-Württemberg, Helmholtz-Gemeinschaft Deutscher Forschungszentren (HGF), Ministerium für Wissenschaft und Forschung, Nordrhein-Westfalen, Ministerium für Wissenschaft, Forschung und Kunst, Baden-Württemberg, Germany; Istituto Nazionale di Fisica Nucleare (INFN), Ministero dell'Istruzione, dell'Università e della Ricerca (MIUR), Italy; Consejo Nacional de Ciencia y Tecnología (CONACYT), Mexico; Ministerie van Onderwijs, Cultuur en Wetenschap, Nederlandse Organisatie voor Wetenschappelijk Onderzoek (NWO), Stichting voor Fundamenteel Onderzoek der Materie (FOM), Netherlands; Ministry of Science and Higher Education, Grant Nos. 1 P03 D 014 30, N202 090 31/0623, and PAP/218/2006, Poland; Fundação para a Ciência e a Tecnologia, Portugal; Ministry for Higher Education, Science, and Technology, Slovenian Research Agency, Slovenia; Comunidad de Madrid, Consejería de Educación de la Comunidad de Castilla La Mancha, FEDER funds, Ministerio de Ciencia e Innovación, Xunta de Galicia, Spain; Science and Technology Facilities Council, United Kingdom; Department of Energy, Contract Nos. DE-AC02-07CH11359, DE-FR02-04ER41300, National Science Foundation, Grant No. 0450696, The Grainger Foundation USA; ALFA-EC / HELEN, European Union 6th Framework Program, Grant No. MEIF-CT-2005-025057, European Union 7th Framework Program, Grant No. PIEF-GA-2008-220240, and UNESCO.

[1] R. Abbasi *et al.* (HiRes Collab.), Phys. Rev. Lett. 100 (2008) 101101 and astro-ph/0703099.
[2] J. Abraham *et al.* (Pierre Auger Collab.), Phys. Rev. Lett. 101 (2008) 061101 and arXiv:0806.4302 [astro-ph].
[3] K. Greisen, Phys. Rev. Lett. 16 (1966) 748.
[4] G. T. Zatsepin and V. A. Kuz'min, Pis'ma Zh. Eksp. Teor. Fiz. 4 (1966) 114.

[5] J. Linsley, Proc of 8th Int. Cosmic Ray Conf., Jaipur 4 (1963) 77.
[6] M. A. Lawrence, R. J. O. Reid, and A. A. Watson, J. Phys. G17 (1991) 733.
[7] M. Nagano *et al.*, J. Phys. G18 (1992) 423.
[8] D. J. Bird *et al.* (Fly's Eye Collab.), Phys. Rev. Lett. 71 (1993) 3401.
[9] A. M. Hillas, J. Phys. G31 (2005) R95.
[10] T. Wibig and A. W. Wolfendale, J. Phys. G31 (2005) 255 and astro-ph/0410624.
[11] V. Berezinsky, A. Z. Gazizov, and S. I. Grigorieva, Phys. Lett. B612 (2005) 147 and astro-ph/0502550.
[12] R. Aloisio, V. Berezinsky, P. Blasi, and S. Ostapchenko, Phys. Rev. D77 (2008) 025007 and arXiv:0706.2834 [astro-ph].
[13] J. Abraham *et al.* (Pierre Auger Collab.), Nucl. Instrum. Meth. A523 (2004) 50.
[14] I. Allekotte *et al.* (Pierre Auger Collab.), Nucl. Instrum. Meth. A586 (2008) 409 and arXiv:0712.2832 [astro-ph].
[15] J. Abraham et al. (Pierre Auger Collab.), submitted to NIM A and 0907.4282 [astro-ph.IM].
[16] J. Abraham et al. (Pierre Auger Collab.), submitted to NIM A.
[17] B. Fick *et al.* (Pierre Auger Collab.), 28th Int. Cosmic Ray Conf., Tsukuba (2003) 449 and astro-ph/0308512
P. Sommers, Astropart. Phys. 3 (1995) 349.
[18] M. Mostafa (Pierre Auger Collab.), Nucl. Phys. Proc. Suppl. 165 (2007) 50 and astro-ph/0608670.
[19] M. Unger, B. R. Dawson, R. Engel, F. Schüssler, and R. Ulrich, Nucl. Instrum. Meth. A588 (2008) 433 and arXiv:0801.4309 [astro-ph].
[20] T. K. Gaisser and A. M. Hillas, Proc. of 15th Int. Cosmic Ray Conf., Plovdiv (1977) 358.
[21] J. Abraham *et al.* (Pierre Auger Collab.), Astropart. Phys. 27 (2007) 155 and astro-ph/0606619.
[22] L. Perrone (Pierre Auger Collab.), Proc of 30th Int. Cosmic Ray Conf., Merida 4 (2007) 331 and arXiv:0706.2643 [astro-ph].
[23] S. Ostapchenko, Phys. Rev. D74 (2006) 014026 and hep-ph/0505259.
[24] S. Ostapchenko, Phys. Lett. B636 (2006) 40 and hep-ph/0602139.
[25] R. S. Fletcher, T. K. Gaisser, P. Lipari, and T. Stanev, Phys. Rev. D50 (1994) 5710.
[26] R. Engel, T. K. Gaisser, T. Stanev, and P. Lipari, Proc. of 26th Int. Cosmic Ray Conf., Salt Lake City 1 (1999) 415.
[27] T. Bergmann *et al.*, Astropart. Phys. 26 (2007) 420 and astro-ph/0606564.
[28] S. Argiro *et al.*, Nucl. Instrum. Meth. A580 (2007) 1485 and arXiv:0707.1652 [astro-ph].
[29] J. Abraham et al. (Pierre Auger Collab.), Phys. Rev. D79 (2009) 171101.
[30] J. Abraham et al. (Pierre Auger Collab.), Astropart. Phys. 31 (2009), 399–406
J. Abraham et al. (Pierre Auger Collab.), Astropart. Phys. 29 (2008), 243.
[31] B. Fick *et al.*, JINST 1 (2006) P11003.
[32] F. Salamida for the Pierre Auger Collab., Proc. 31th Int. Cosmic Ray Conf. (Lodz, Poland) (2009) and 0906.2189 [astro-ph.HE].
[33] M. Nagano, K. Kobayakawa, N. Sakaki, and K. Ando, Astropart. Phys. 20 (2003) 293 and astro-ph/0303193.
[34] M. Ave *et al.* (AIRFLY Collab.), Astropart. Phys. 28 (2007) 41 and astro-ph/0703132.
[35] H. M. J. Barbosa *et al.*, Astropart. Phys. 22 (2004) 159–166 and astro-ph/0310234.
[36] T. Pierog, R. Engel, D. Heck, S. Ostapchenko, and K. Werner, Proc. of 30th Int. Cosmic Ray Conf., Merida 4 (2007) 625.
[37] R. Knapik *et al.* (Pierre Auger Collab.), Proc of 30th Int. Cosmic Ray Conf., Merida 4 (2007) 343 and arXiv:0708.1924 [astro-ph].
[38] S. Y. BenZvi *et al.*, Nucl. Instrum. Meth. A574 (2007) 171 and astro-ph/0609063.
[39] B. Keilhauer *et al.* (Pierre Auger Collab.), Proc. of 29th Int. Cosmic Ray Conf., Pune 7 (2005) 123 and astro-ph/0507275.
[40] S. Y. BenZvi *et al.* (Pierre Auger Collab.), Proc of 30th Int. Cosmic Ray Conf., Merida 4 (2007) 355 and arXiv:0706.3236 [astro-ph].
[41] C. Di Giulio for the Pierre Auger Collab., Proc. 31th Int. Cosmic Ray Conf. (Lodz, Poland) (2009) and 0906.2189 [astro-ph.HE].
[42] A. Castellina for the Pierre Auger Collab., Proc. 31th Int. Cosmic Ray Conf. (Lodz, Poland) (2009) and 0906.2319 [astro-ph.HE].
[43] R. U. Abbasi *et al.* (HiRes Collab.), Astropart. Phys. 32 (2009) 53–60.
[44] http://www.auger.org/combined_spectrum_icrc09.txt